International Journal of Thin Film Science and Technology

Volume 4
Issue 2 *May 2015*

Article 3

2015

Relation between Microstructure and Electric Resistivity of Copper, Nickel, NixCu1-x Alloys and Ni/Cu Bilayered Thin Films.

M. K. Loudjani
Laboratoire de Thermodynamique et Physico-Chimie des Hydrures et Oxydes, Bât. 415, Université Paris-Sud-XI ,15 Rue Georges Clemenceau, 91505 Orsay Cedex, France, mohamed-khireddine.loudjani@u-psud.fr

C. Sella
Institut des Nano-Sciences de Paris, Université de Paris-VI, campus Boucicaut, 140 rue de Lourmel 75015 Paris, France, mohamed-khireddine.loudjani@u-psud.fr

Follow this and additional works at: https://digitalcommons.aaru.edu.jo/ijtfst

Recommended Citation

K. Loudjani, M. and Sella, C. (2015) "Relation between Microstructure and Electric Resistivity of Copper, Nickel, NixCu1-x Alloys and Ni/Cu Bilayered Thin Films.," *International Journal of Thin Film Science and Technology*: Vol. 4 : Iss. 2 , Article 3.
Available at: https://digitalcommons.aaru.edu.jo/ijtfst/vol4/iss2/3

This Article is brought to you for free and open access by Arab Journals Platform. It has been accepted for inclusion in International Journal of Thin Film Science and Technology by an authorized editor. The journal is hosted on Digital Commons, an Elsevier platform. For more information, please contact rakan@aaru.edu.jo, marah@aaru.edu.jo, u.murad@aaru.edu.jo.

International Journal of Thin Films Science and Technology

http://dx.doi.org/10.12785/ijtfst/040203

Relation between Microstructure and Electric Resistivity of Copper, Nickel, Ni_xCu_{1-x} Alloys and Ni/Cu Bilayered Thin Films.

M. K. Loudjani [1,*] and *C. Sella* [2].

[1] Laboratoire de Thermodynamique et Physico-Chimie des Hydrures et Oxydes, Bât. 415, Université Paris- Sud-XI ,15 Rue Georges Clemenceau, 91505 Orsay Cedex, France

[2] Institut des Nano-Sciences de Paris, Université de Paris-VI, campus Boucicaut, 140 rue de Lourmel 75015 Paris, France

Received: 15 Oct. 2014, Revised: 1 Apr. 2015, Accepted: 2 Apr. 2015.
Published online: 1 May 2015.

Abstract: In this study we compare the influence of the microstructure and of chemical composition on resistivity of pure metals of Cu and Ni, Ni_xCu_{1-x} alloys as well as Ni/Cu bilayered films. When the distance between defects becomes comparable or smaller than the wavelength associated to the conduction electron mean free path and when these defects are randomly distributed the resistivity increases by several orders of magnitude. The resistivity of a Ni_xCu_{1-x} alloy film is approximately 10 times larger than the resistivity of a Ni/Cu bilayered film having the same mean atomic composition.

Keywords: Ni_xCu_{1-x} alloys films, resistivity of bilayered films Ni/Cu, Interface-resistivity, and order-disorder.

1 Introduction

It is well-known that at ambient temperature the bulk resistivity of polycrystalline alloys can be written in the following form: $\rho = \rho_T + \rho_I + \rho_R$. The three terms in this expression represent the three classes scattering mechanisms which are respectively: phonons (ρ_T), chemical impurities (ρ_I), and defects related to the microstructure (grain boundary, surfaces and interfaces.., ρ_R). Nordheim [1] developed one of the first theoretical model taking into account the effects of chemical impurities. In the case of thin metallic film the resistivity, according to the models' developed by Fuchs- Sondheimer (F-S) [2-3] and by Mayadas-Shatzkes (M-S) [4], depends on the film thickness, electron mean free path, mean grain size, electronic properties of the film surface scattering and grain boundaries.

To analyze the effects at a nanometric scale of microstructural defects and chemical composition [5-8] on the film resistivity, the resistance measurement using the method of in-line four points' probes was used. The studied metal samples having an f.c.c structure: copper, nickel, Ni/Cu bilayers and Ni_xCu_{1-x} alloys are deposited on to insulating substrates. Bulk samples of these metals and alloys used as references standards of these materials were analyzed.

In order to compare the contribution to the resistivity of each class of defects, we prepared Ni/Cu bilayered films of various thicknesses and Ni_xCu_{1-x} alloys films with an average composition is the same as that of the bilayered sample. In the case of Ni/Cu bilayered films, we applied the model developed by Schumann-Gardner (S-G) [9-10] to calculate the resistivity related to the interface between Ni and Cu.

The influence of the defects density on the resistivity before and after annealing of bulk Cu, Ni and Ni_xCu_{1-x} alloys was studied and compared to the results obtained with Cu, Ni, and Ni_xCu_{1-x} alloy films. Besides the resistivity of Ni_xCu_{1-x} alloy films was compared with the resistivity of Ni/Cu bilayered films of the same mean composition.

Various techniques including, X-rays diffraction (X.R.D) and Transmission Electronic Microscopy (T.EM.) were used to elucidate the relative contribution of various classes of defects and their spatial distribution on the resistivity of thin films.

2 Preparation of thin films

The thin films were prepared by R.F. sputtering from a disk-shaped target of 13 cm in diameter with a target substrate distance of about 4 cm. The base pressure of the vacuum chamber was 1.3310^{-4} Pa and sputtering took place

*Corresponding author e-mail: mohamed-khireddine.loudjani@u-psud.fr

© 2015 NSP
Natural Sciences Publishing Cor.

in an argon atmosphere at a pressure of 1.33 Pa. Before deposition, the target was subjected to a presputteing. During this presputtering time (15 to 30 mn) the substrate was protected by a shutter. The substrates consist of 1737 corning glass disks (30.5 mm diameter and 1 mm thick). The deposition rate of copper and nickel films are respectively 1.94 $Å.s^{-1}$ and 3.54 $Å.s^{-1}$. During the preparation of films, the second layer is deposited after that the first layers was exposed to air. The thicknesses of films are reported in Table-1. The microstructure of the films was studied by TEM on samples deposited on to carbon films supported by fine copper mesh.

3 Electrical Measurements

In this study we used a power source (KEITHLEY-2400) to supply a D.C. current to the two external probes and a nanovoltmeter (KEITHLEY-2182A) to measure the voltage between the two internal probes, Fig.1. Each test of measurements is carried out by imposing automatically an alternate pulse sweeping while running of increasing heights, and variable in the interval, I = - 40 mA with I = 40 mA. The current is applied during 40 ms. Measurements of the levels of the differences in tensions between the two internal probes are taken after approximately 36 ms, after initiating the current pulses. The resistance of film between the two internal probes is given from the slope of the V (I) variation. Measurements are performed vacuum (P ≈ 1.5 Pa) and at ambient temperature T = 293 K.

The calculation of the resistivity is deduced from the measured resistances by using the models developed by Smits [11] in the case of a homogeneous layer deposited on an insulator substrate, and the model of Schumann-Gardner in the case of the conducting bilayered films.

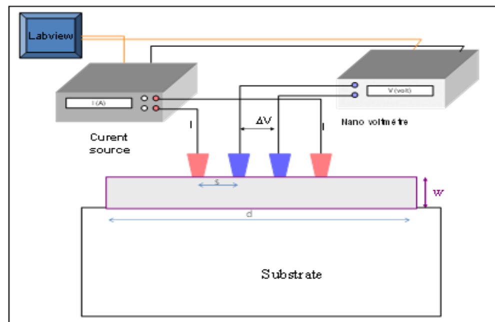

Fig. 1 Principle of measurement of electric resistance by four point's method

In the case of thin films of thickness w, with w << s, the resistivity of a sample having the shape of a disk shaped sample of diameter d is connected to the resistance by the relation of Smits: $\rho = R.C.w$ (1a), C is the geometrical correction factor given by the following relation (1b) and s was the probe separating distance:

$$C = \frac{\pi}{\ln 2 + \ln\left(\frac{\left(\frac{d}{s}\right)^2 + 3}{\left(\frac{d}{s}\right)^2 - 3}\right)} \quad (1b)$$

The model of Schumann-Gardner was developed in the case of the diffusion layer of single-phase material divided into n layers, and presenting a gradient of resistivity in the whole layer thickness. In the case of a layer divided into n layers, the electric potential at a point M(r, z) of the $n^{ième}$ layer is determineted by Schumann-Gardner in cylindrical co-ordinates. r is the distance from the probe and z the depth measured from surface of the first layer. The extremity of each probe is of finite size, it has a circular surface contact of radius a with the first layer, Fig.2. The potential in a point of $n^{ième}$ layer is given by the expression:

$$V_n(r,z) := \int_0^\infty \theta_n(\lambda)\, J_0(\lambda\, r)\, \mathbf{e}^{(-\lambda z)}\, d\lambda + \int_0^\infty \psi_n(\lambda)\, J_0(\lambda\, r)\, \mathbf{e}^{(\lambda z)}\, d\lambda \quad (2)$$

$J_0(\rho\lambda)$ is the function of Bessel of first species of order zero, a the contact radius of the probe, $\psi_n(\lambda)$ and $\theta_n(\lambda)$ two functions which depend on the boundary conditions and the initial conditions (the number of layers, the thicknesses of the layers, the resistivities of the different layers, and the shape of the current density distribution at the end of each current probe).

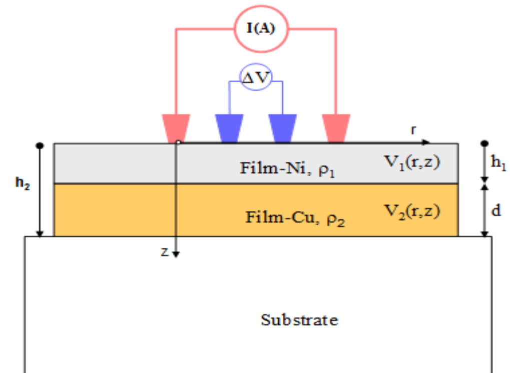

Fig. 2 Principle of measurement of spread resistance of Ni/Cu bilayered films.

In the case of a system with two layers having a contact resistance at the interface between the first and the second layer, the condition of continuity of the current density in the S-G model is replaced by the condition [12]:

$$V_1(r, z = h_1) - V_2(r, z = h_1) = -J.\rho_I$$

The expressions of the potentials at the two points of measurements of surface external and located respectively at the distances r = s, and r = 2s of the probes of current are

© 2015 NSP
Natural Sciences Publishing Cor.

given by:

$$V_1(r=s, z=0) = \frac{I_0 \rho_1}{2\pi a} \int_0^\infty \frac{(1+2\theta_1(\lambda)\sin(\lambda a)(J(0,\lambda s)}{\lambda} d\lambda , \quad (3a)$$

$$V_1(r=2s, z=0) = \frac{I_0 \rho_1}{2\pi a} \int_0^\infty \frac{(1+2\theta_1(\lambda)\sin(\lambda a)(J(0,2\lambda s)}{\lambda} d\lambda \quad , (3b)$$

The function $\Theta_1 = 1 + 2\theta_1$ is written:

$$\Theta_1 = \frac{N_1 + N_2}{D_1 + D_2} \quad (3c),$$

With

$$N_1 = -e^{(z\lambda - 2h_2\lambda)}(\rho_1 + \rho_2 - \lambda\rho_I) + e^{(-2d\lambda - z\lambda)}(\rho_1 - \rho_2 + \lambda\rho_I) , \quad (3d)$$

$$D_1 = e^{-2h_2\lambda}(\rho_1 + \rho_2 - \lambda\rho_I) + e^{(-2d\lambda)}(\rho_1 - \rho_2 + \lambda\rho_I) , \quad (3e)$$

$$N_2 = e^{(z\lambda - 2h_1\lambda)}(\rho_1 - \rho_2 - \lambda\rho_I) - e^{(-z\lambda)}(\rho_1 + \rho_2 + \lambda\rho_I) , \quad (3f)$$

$$D_2 = e^{-2h_1\lambda}(\rho_1 - \rho_2 - \lambda\rho_I) - (\rho_1 + \rho_2 + \lambda\rho_I) , \quad (3g)$$

I_0 *is the intensity of the current delivered by each of the two probes,* ρ_1 is the resistivity of the first layer (nickel) located at the depth z = 0, ρ_2 the resistivity of the second layer (copper), ρ_I represents the resistivity of the interface between the two layers Ni/Cu, h_1 and h_2, are respectively the depths of the interfaces limiting the two layers, and d = h_2 - h_1 the thickness of the second layer of copper.

The potential difference measured between the two internal probes, $\Delta V = V_1(0,s) - V_1(0,2s)$, as well as the electric resistance between these two probes are respectively equal to:

$$\Delta V = \frac{I_0 \rho_1}{2\pi a} \int_0^\infty \frac{\sin(\lambda a)(1+2\theta_1(\lambda)(J(0,\lambda s) - J(0,2\lambda s))}{\lambda} d\lambda, \quad R = \frac{\Delta V}{I_0} \quad (4)$$

To calculate this integral numerically we used the method of approximation of Simpson, using Maple software.

4 Relation Between Microstructure and Electric Properties in Bulk Materials and Thin Films

4.1 Bulk properties

The resistivities of standard bulk samples measured on copper, nickel and Constantan alloy (99.9% purity) with an atomic composition of $Cu_{53}Ni_{47}$ (from Goodfelow). The samples are disks (25 mm diameter and 20 µm thickness). The electrical measurements are taken on the samples in their rough structural state and after an annealing during one hour under vacuum in order to obtain as structural reference the recristallized unconstrained state of each material. The temperatures of annealing are respectively T = 451°C for copper, T = 522°C for the $Cu_{53}Ni_{47}$ alloy and T = 603°C for Nickel. To insulate electrically the samples during measurement and to avoid their deformation during handling, the disks are stuck on glass substrates.

The evolution of the grains size with annealing, was studied from the broadening of the X-ray (111) diffraction peak by using the relation of Debye-Scherrer (5) and by neglecting the term of widening due to the deformations:

$$B = \frac{0.9\lambda}{\phi \cos(\theta B)} \quad (5)$$

With ϕ the average particle size λ_{Cu} = 1.5405 Å the wavelength of the copper-$K_{\alpha 1}$ line and θ_B the Bragg angle. The relative variation of the grains size between the two structural states of the standard materials is less than 10% (Table-1).

The electrical measurements presented on Table-1 and Fig.3, show a slight drop of resistivity of the materials after annealing. In the case of nickel, and in spite of an important variation of the grains size, the resistivity varies slitghtly. For this class of grains sizes of $\phi \geq 40$ nm, the relative variation of the resistivity between the two structural states (annealed and unannealed) of the standard materials is less than 10%.

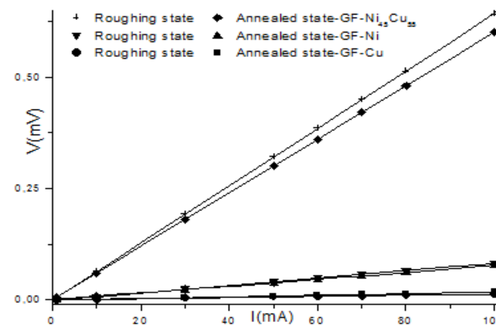

Fig. 3 Annealing effect and alloying effect on the resistance of the standard samples (copper, nickel and $Ni_{47}Cu_{53}$ alloy).

4.2 Experimental results on thin film materials

Microstructure of nickel and copper films:

The grains size of as deposited films obtained by TEM, Fig.4a, 4b, and XRD, Fig.4a-b. The grains size of copper films appears very heterogeneous and the crystals present an important proportion of twin boundaries [15].

© 2015 NSP
Natural Sciences Publishing Cor.

The grains in nickel film are much smaller than those in copper film. The size of grains determined by (TEM), according to the direction perpendicular to the film surface, is about 10 ± 3 nm for nickel films, (Fig.4a), and about 30 ± 15 nm for copper films, (Fig.4b). These sizes of grains are smaller than the thicknesses of corresponding films.

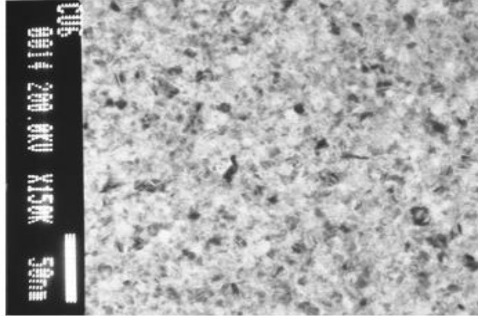

Fig. 4 (a) Nickel film thickness = 47 ± 5 nm.

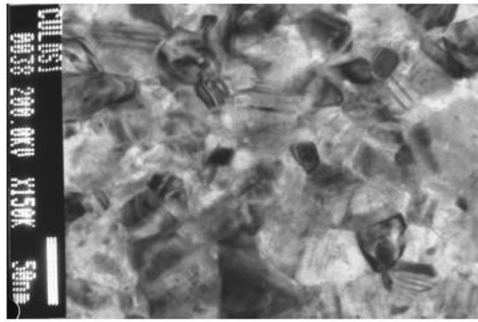

Fig. 4 (b) Copper film thickness = 85 ± 5 nm.

As indicated in Fig.5 the diffraction spectrum carried out on as deposited films shows the existence of an anisotropy of crystalline orientation with the presence of only one peak (111) of significant intensity. The annealing of films decreases this anisotropy and reveals additional orientations (220), Fig.5b. In copper as deposited films the grain size obtained from the broadening of the X-ray (111) diffraction peak, is smaller than the size of the grains observed by TEM. In the case of the nickel films the sizes determined by the two methods are comparable.

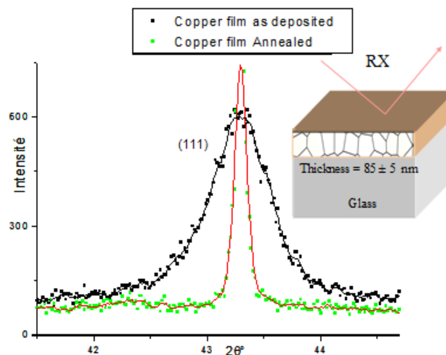

Fig. 5 (a) Effect of annealing on the broadening of the X-ray (111) diffraction peak.

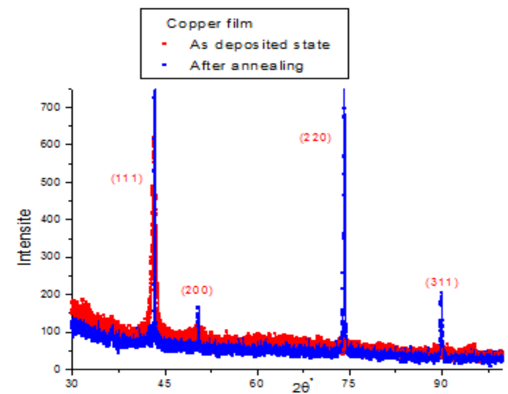

Fig. 5 (b) Effect of annealing on the anisotropy of crystalline orientation in copper films.

Electrical measurements on thin films:

Effect of thickness and of annealing on the resistivity of metal films:

Figures-6-7 shows the *dependence* of variations of resistances and the resistivities of nickel and copper films, with the thickness of films, before and after a 90 minutes vacuum annealing at 498°C. One notices on these figures and on the table-1 a stronger relative drop of the resistivity after annealing of nickel films compared to copper films. The important concentration of defects and the low size of grains are at the origin of this variation. The elimination of an important proportion of point defects during thermal annealing and an increasing of the grain size result in a significant decrease of the resistivity.

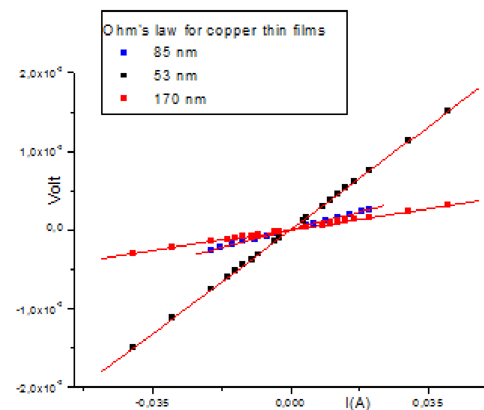

(a) Copper films.

© 2015 NSP
Natural Sciences Publishing Cor.

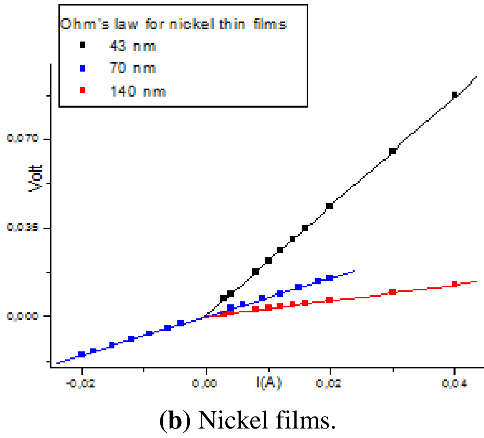

(**b**) Nickel films.

Fig.6: V(I) curves for different thicknesses of copper (**a**) and nickel (**b**) films.

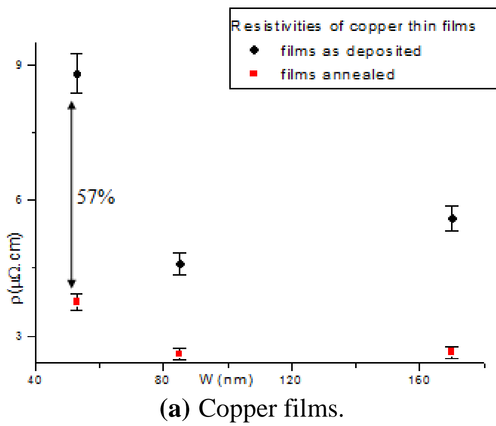

(**a**) Copper films.

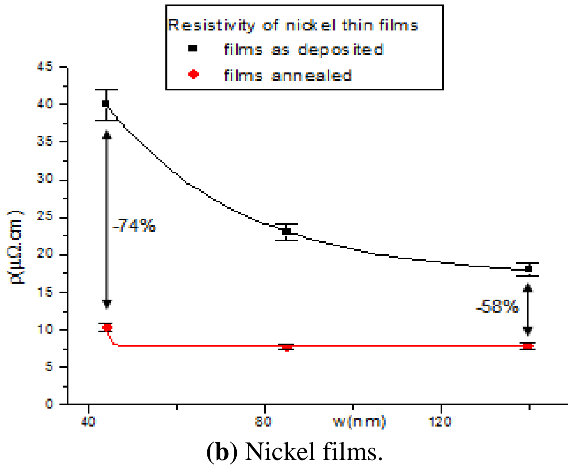

(**b**) Nickel films.

Fig. 7: Effect of annealing at 498°C and films thickness on the resistivitiy of (**a**) copper and (**b**) nickel

In the model developed by F-S [4-5], the three physical-chemical parameters controlling the resistivity of thin films are: the thickness of films w, the nature of the electronic scattering on the surfaces of films, characterized by the parameter p, and the mean free path of conduction electronsλ. According to this model the resistivity of the thin film samples ρ_{FS} when the thickness becomes comparable or smaller than the electron mean free path the resistivity is given par.

$$\rho_{FS} = \rho_b[1 - \frac{3}{8}\frac{\lambda}{w}(1-p)\int_1^\infty (\frac{1}{x^3} - \frac{1}{x^5})(\frac{1-e^{-\frac{w}{\lambda}x}}{1-pe^{-\frac{w}{\lambda}x}})dx]^{-1} \quad (6)$$

ρ_b is the resistivity of the bulk materials, p the probability that an electron will be specularly reflected upon scattering from a film surface and takes a values from 0 to 1.

This model was supplemented by that proposed by M-S [6] in the case of *polycrystalline films* by introducing into the expression of the resistivity two additional parameters characterizing the *microstructure of* films: the average grain size ϕ supposed to be close to the film thickness, and the grain boundary reflection coefficient R. The expression of the resistivity ρ_{MS} according to this model becomes:

$$\rho_{MS} = \frac{\rho_{FS}}{MS},$$

with , with (7)

$$MS(\alpha) = 3\left[\frac{1}{3} - \frac{\alpha}{2} + \alpha^2 - \alpha^3 \ln(1+\frac{1}{\alpha})\right] \qquad \alpha = \frac{\lambda R}{\phi(1-R)}$$

We applied these two models, F-S and M-S, to determine the physical parameters R, ϕ, p and λ, to nickel and copper films after thermal annealing, Table-2. The first remark that we can follow upon these results is that model F-S and M-S was applicable to copper and nickel films deposited on a substrate with an agreement of about 10%.

In the case of copper films these parameters obtained by fitting of the relative experimental resistivities, $(\rho_f/\rho_b)_{exp}$, are gathered in the Table-2. The average grain size ϕ deduced from this model are approximately half the thicknesses of films determined by TEM but of the same order of magnitude as those determined by X-ray diffraction. The parameter λ remains almost constant when the thickness of the film increases. Its value lies between two and three times the electron mean free path in the copper calculated according to the Sommerfeld theory assuming the usual one conduction electron per atom: $\lambda_{Cu} = \frac{2^{2/3} h a_{Cu}{}^2}{8\rho_{Cu} e^2} \approx 42.8nm$ where h is the Planck's constant, e the electronic charge, ρ_{Cu} the resistivity of the copper and $a_{Cu} \cong 3.62$ Å the cell parameter of copper. The value of the parameter p_{Cu} is close to zero, assuming that the surface scattering of electrons has a non-specular character. The grain boundaries reflections coefficients R_{Cu} of this work are lower than those given by M-S and seem

© 2015 NSP
Natural Sciences Publishing Cor.

to increase with the thickness.

In the case of nickel films the fitting parameters given, show an average grain sizes of the same order of magnitude as the thicknesses of corresponding films. As for the parameter λ they remain about constant for the three thicknesses of films considered and is approximately three times the electron mean free path in the massive nickel, calculated with the same model and assuming 0.6 electron conduction per atom according to Mott studies [13]: $\lambda_{Ni} = \frac{0.279ha^2}{\rho_{Ni}e^2} \approx 13.5nm$, where $a_{Ni} \cong 3.52$ Å is the cell parameter of nickel and ρ_{Ni} its resistivity. The values of the parameters, p_{Ni} and R_{Ni}, for the nickel films are close to zero and do not vary with film thickness.

4.3 Interface resistivity of a Nickel/copper bilayer:

Spread resistances R_S measured, according to Fig.2, on the external surface of a Ni/Cu bilayer, and those calculated according to the model of Schumann and Gardner (eq-4) are given in Table-3. The average resistivity of interface determined by this method for the three studied bilayers is: $\rho_I = (0.4 \pm 0.2)$ mΩ.cm^2. This average value is obtained by fixing the geometrical parameters to: a = 0.3 µm and s = 2.54 mm, and by adjusting in the equations (3a-3d) the parameters d, h_1, ρ_1 and ρ_2, characterizing the bilayer with less than 10% close to the experimental values obtained on copper and nickel films: d = w_{Cu}, h_1 = w_{Ni}, $\rho_1 = \rho_{Ni}$ and $\rho_2 = \rho_{Cu}$. By this method the calculated spread resistance R_S agrees with the experimental value within less than 2%.

5 Role of the Chemical Disorder on the Resistivity of Alloys

In order to compare the contributions of various defects: points defects, chemical composition, grain boundary, surfaces, and interfaces on the resistivity two types of $Cu_{1-x}Ni_x$ alloys films were prepared:

- On one hand two solid solutions alloys with atomic compositions of $Cu_{67.3}Ni_{32.7}$ and $Cu_{53.1}Ni_{46.9}$ with respective cell parameters: a_1 = 0.357 nm and a_2 = 0.358 nm. For these strong nickel concentrations the average distance between chemical impurities is close the wavelength, $\lambda_{Cu} \approx 0.457$ nm, associated with the electrons whose energy is equal to the Fermi energy in copper.

- in addition, three Ni/Cu bilayers with thicknesses selected in order to obtain average atomic compositions per unit of volume of copper and nickel equivalent to those in alloy films $Cu_{67.3}Ni_{32.7}$ and $Cu_{53.1}Ni_{46.9}$.

From a comparison of the results given in the figures Fig.8a-8b-8c and Tables-1-3, one can deduce the two classes from defects controlling the resistivity: microstructural defects and chemical impurities their spatial distribution on one hand, the thickness and average size of the grains on the other hand. When in each class of defects the average distance between electronic scattering centers becomes close or smaller than the average wavelength associated the electrons of conduction the resistivity grows and tends towards a maximum when this length approaches the wavelength associated to the conduction electrons having the Fermi energy.

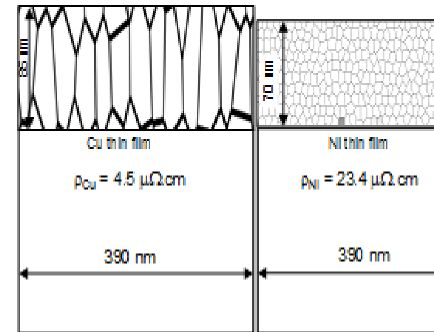

(a) Microscopic scale

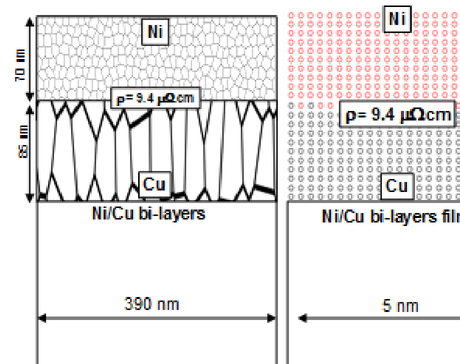

(b) Micro-nanoscopic scale

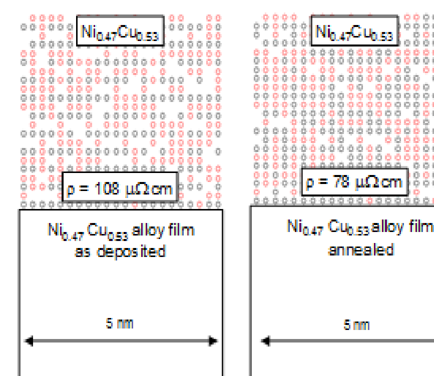

(c) Nanoscopic scale

Fig.8: Effect of different defects (microstructure, random distribution of the chemical composition) compared to the bilayer structure on the resistivity of Cu, Ni, $Ni_{47}Cu_{53}$ alloy and Ni/Cu bi-layers films.

© 2015 NSP
Natural Sciences Publishing Cor.

When in Ni_xCu_{1-x} system one goes from a fcc alloy lattice with a random spatial distribution of the chemical elements (Cu and Ni) to a bilayer Ni/Cu, of two pure Ni and pure Cu fcc lattices, the apparent resistivity of the bilayer is approximately 92% weaker than in the case of Ni_xCu_{1-x} alloy see Table-3. After thermal annealing the resistivity of alloy films decreases only by 23% of its initial value.

Table 1: Thicknesses, average gain size (obtained by X-ray diffraction and by T.E.M), resistivity (before and afterthermal annealing) of bulk samples and thin film of copper, nickel and Cu_xNi_{1-x} alloys.

Samples	Materials	Structural state	Thicknesses films (nm)	Bragg- angle 2θ°	Grain size (ϕ, nm) by X.R.- diffraction	Grain size (ϕ, nm) by T.E.M.	Resistivity ρ(μΩ.cm)	$\frac{\Delta\phi}{\phi}$ (%)	$\frac{\Delta\rho}{\rho}$ (%)
Standard samples (Bulk)	Ni	Rough Annealed	2.10[4] nm	44.38 44.41	40 41	Not determineted	6.97 6.61	2.5	- 5.2
	Cu	Rough Annealed		43.22 43.23	66 85		1.64 1.57	2.9	- 4.3
	$Ni_{0.47}Cu_{0.53}$	Rough Annealed		43.88 43.86	47 52		52.75 49.09	10.6	- 6.9
Thin films samples	Ni	As deposited Annealed	24 - -	44.54		As deposited 10 ± 3	61.9 - -		- 85.4
		As deposited	44 - -				40 10.3		
		As deposited Annealed	70 - -		9.5 43		23.3 7.7	353	- 67
		As deposited Annealed	140 - -				18.8 8.8		- 53.2
	Cu	As deposited Annealed	53 - -			As deposited 30 ± 15	8.5 3.7		- 56.5
		As deposited Annealed	85 - -	43.276	14 20		4.5 2.6	43	- 42.2
		As deposited Annealed	170 - -				5.6 2.6		- 53.6
	$Ni_{0.47}Cu_{0.53}$ (AL1)	As deposited Annealed	208 - -	43.81	- - 31.6	10	108 78		- 27.8
	$Ni_{0.367}Cu_{0.67.3}$ (AL2)	As deposited Annealed	214 - -	43.65 - -	- - 33.6	11.9	88.9 68.2		- 23.3

Table 2: Table 2: Fitting parameters R, ϕ, λ and p, according to F-S and M-S models, for the annealed films of copper and nickel.

Materials	Standard samples annealed		Thin films samples annealed							
	Thickness (nm)	Bulk resistivity ρ(μΩ.cm)	Simulation of parameters Models- (F.S-M.S)				Comparison experiment and model (F-S-M-S).			
			$R_{ef.}$	ϕ (nm)	λ (nm)	P	Thickness (nm)	$\left(\frac{\rho_{film}}{\rho_{Bulk}}\right)$ Experience	$\left(\frac{\rho_{film}}{\rho_{Bulk}}\right)_{FSMS}$ model (F.S-M.S)	Variation
Cu	2.10[4] nm	1.57	0.03	20	100	0.05	53	2.34	2.21	Δ = 6 %
			0.11	80			85	1.66	1.83	Δ = 10 %
			0.13	100			170	1.69	1.52	Δ = 10 %
Ni		6.61	0.01	43	100	0.05	44	1.56	1.46	Δ = 6 %
			0.03	85			70	1.16	1.28	Δ = 10 %
			0.03	127			140	1.2	1.15	Δ = 4 %

6 Conclusion

This study highlights the role of the various classes of defects on the electric properties of thin film: The disorder related to the chemical composition or to the interfaces has an influence on the resistivity only if the spatial scale of their distribution is of the order of electrons conduction mean free path. When the average grain size is larger than the electron mean free path the effect of grain boundaries on the resistivity is negligible. In this case the variation of the resistivity of films, according to the

© 2015 NSP
Natural Sciences Publishing Cor.

thickness, follows the models suggested by F-S and M-S. The conduction electron mean free path determined in

Table 3: Comparison of the experimental and calculated thicknesses (w_{Ni}, w_{Cu}), resistivity (ρ_{Ni}, ρ_{Cu}, ρ_{BL}), spread resistance (R_S), interface resistivity (ρ_I) characterizing the Ni/Cu bilayered films.

	Materials		**Experiment**						**Interface resistivity between nickel and copper in bilayered films** ρ_I**(mΩ.cm²)**	**Relative variation between resistivity in** Ni_xCu_{1-x} **films alloys (AL1, AL2) and in Ni/Cu bilayered films (BL1, BL2, BL3)** $\frac{\rho_{BL}-\rho_{Asd}}{\rho_{Asd}}$
			Films thicknesses w_{Ni}, w_{Cu}, $w_{Ni}+w_{Cu}$		**Resistivity (μΩ.cm)** ρ_{Ni}, ρ_{Cu},	**Bulk Composition**	**Spread Resistance** R_S**(Ω)**	**Bilayered resistivity** $\rho_{BL}=R_S*w*C$		
Bilayered Ni/Cu films as deposited (BL)	BL1	Ni Cu	24 53	77	61.9 8.8	$Ni_{0.327}Cu_{0.673}$	0.366 Ω	12.0		
	BL2	Ni Cu	70 85	155	23.4 4.5	$Ni_{0.469}Cu_{0.531}$	0.142 Ω	9.4		
	BL3	Ni Cu	140 170	310	18.8 5.6	$Ni_{0.469}Cu_{0.531}$	0.066 Ω	8.7		
			Simulation (S-G model)							
			Films thicknesses (nm)		Resistivity (μΩ.cm)	Bulk composition	Spread resistance (Ω)	ρ_{BL}(μΩ.cm)		
	BL1	Ni Cu	22.5 49.5	72	63 8.8	$Ni_{0.328}Cu_{0.672}$	0.367 Ω	11.3	0.2	- 89 %
	BL2	Ni Cu	69 82	151	23 6.5	$Ni_{0.475}Cu_{0.525}$	0.141 Ω	9.1	0.4	
	BL3	Ni Cu	135 165	300	18.8 6	$Ni_{0.468}Cu_{0.532}$	0.066 Ω	8.5	0.5	- 92

copper and nickel thin films, from the models FS-MS, at the ambient temperature, is larger than that of the corresponding bulk materials.

When the density of randomly distributed defects increases, with an average distance between the electronic scattering centers comparable with electrons mean free path having an energy close to Fermi level, the resistivity increases several orders of magnitude. When in the solid solution Ni_xCu_{1-x} one goes from a system where the spatial distribution of the chemical elements “coppers and nickel” in the crystal lattice is random to a completely ordered system corresponding to Ni/Cu bilayer, the resistivity varies approximately by 92%. Finally in Ni/Cu bilayer films, the resistivity associated with the interface between nickel and copper layers is of several orders of magnitude larger than the resistivity of interfaces related to the grain boundaries.

Acknowledgements

The autors wish to acknowledge the staff of the Department M.P-IUT-Orsay, of ICMMO-Université-Paris-Sud-XI-Orsay of INSP-Boucicaut-Paris-VI and CECM-Vitry who contributed to various stages of this study.

Reference

[1] Nordheim, L. 1934, *Act. Sci. Et Ind.* N°. 131 (Paris: Hermann).

[2] K. Fuchs, *Proc. Camb. Phil.*, Soc., **34**, 100, (1938).

[3] E.H. Sondheimer, *Advances in Physics* Vol.**1**, N°1, 1-42, (1952).

[4] F. Mayadas, M. Shatzkes, *Phy. Rev*. B, Vol.**1**, N°4, 1382-1389, (1970).

[5] R. Smoluchowski, *Phys. Rev* Vol. **84**, N°3, 511-518, (1951).

[6] Yeong Der Yao, J. H. Tsai, *Chinese Journal of Physics*, Vol. **16**, N°4, 189-195, (1978).

[7] V.F. Gantmkher, Electrons and Disorder in Solids Clarendon Press Oxford, (2005).

[8] R. Coehoorn, *Novel Magnetoelectronic Materials and devices*, Lecture Notes TU/e 2001-2002.

[9] P.A. Schumann, Jr. and E.E. Gardner, *J. Electrochemical. Soc. Solid State Science and Technology*, vol. **116**; N°1, pp. 87-91, (1969).

[10] P.A. Schumann, Jr. and E.E. Gardner, *Solid-state Electronics*, vol. **12**, pp. 371-375 (1969).

[11] F. M. Smits, Measurement of sheet resistivities with the four point probe, *The Bell System technical journal*, pp.711-717, (1958).

[12] C. W. Wang, K. A. Cook and A. M. Sastry, *J. Electrochemical. Soc.*, **150**, (3), A385-A397 (2003).

[13] N. F. Mott, *Proc. Phys. Soc.* **47**, 571-588, (1935).

© 2015 NSP
Natural Sciences Publishing Cor.